

# Time evolution of gluon coherent state and its von Neumann entropy in heavy-ion collisions

Hideaki Iida and Teiji Kunihiro

*Department of Physics, Kyoto University, Kyoto 606-8502, Japan*

Akira Ohnishi

*Yukawa Institute for Theoretical Physics, Kyoto University, Kyoto 606-8502, Japan*

Toru T. Takahashi

*Gumma National College of Technology, Gumma 371-8530, Japan*

We propose a new prescription for evaluating a von Neumann entropy in the initial stage of high-energy heavy-ion collisions utilizing the time evolution of classical Yang-Mills (CYM) field: The von Neumann entropy is computed for the quantum coherent states constructed so as to give the classical gluon fields as the expectation values. The entropy is to be liberated when the complete decoherence is achieved. As a demonstration, the time evolution of the CYM dynamics is solved with an initial condition which mimics the Glasma state, though in a non-expanding geometry; the Glasma state is characterized by the longitudinal color-electric and -magnetic fields with gluon fields' fluctuations around it. We find that the initial longitudinal fluctuations of the fields play essential roles for the entropy production in two ways: First, the field fluctuations at  $t = 0$  themselves act as a source of the von Neumann entropy prepared before the time evolution. Second, the initial fluctuations triggers field instabilities, and hence the larger the strength of them, the more the entropy production at later time.

## I. INTRODUCTION

Experiments with high-energy heavy-ion collisions (HIC) in Relativistic Heavy-Ion Collider (RHIC) at Brookhaven National Laboratory and Large Hadron Collider (LHC) at CERN revealed interesting properties of created hot matter called the Quark-Gluon Plasma (QGP). One of the curious properties found in HIC experiments is the early thermalization; the thermalization time is estimated to be  $\tau_0 \simeq 1.0$  fm/c from the analysis of the data obtained by RHIC using relativistic hydrodynamic equations [1, 2]. This thermalization time is considerably smaller compared with the prediction by perturbative QCD [3]. To tackle the problem, we need to understand the non-equilibrium QCD dynamics starting from the realistic initial condition for HIC.

The key issues for elucidating the possible mechanism of the early thermalization are how and when entropy is produced in the early stage of HIC. Nuclear wave functions before the collision are considered to be described by the color glass condensate caused by the gluon saturation [4–6], where the (semi-)classical approximation is valid [7–9]. The matter created just after the collision of two nuclei has a specific configuration of the fields called ‘‘Glasma’’ [6], where color-electric and -magnetic fields are aligned parallel to the collision axis between two colliding nuclei. It is suggested that the Glasma state induces some instabilities, i.e., Weibel and Nielsen-Olesen instabilities [10, 11], which may cause isotropization at early time, and hence hopefully thermalization [12–15]. One should, however, note that the matter which can be well described by the dissipative hydrodynamics does not necessarily have isotropic particle distribution.

A direct examination of the entropy production in the early stage of HIC is done in Refs. [16, 17], where Kolmogorov-Sinaï (KS) entropy is given as the sum of the positive Lyapunov exponents calculated through solving the time evolution of CYM; the positive Lyapunov exponents and thus Kolmogorov-Sinaï (KS) entropy represent the mixing property of the system. See [18–24] for early investigations of the chaotic behavior of CYM. In Ref. [17], the authors solved the equation of motion of CYM starting from Glasma-like initial conditions, and found a large number of positive Lyapunov exponents in the early stage when the initial field fluctuations are included, and even for later times their number is a sizeable fraction of the total number of degrees of freedom, indicating a significant amount of entropy is produced by *classical gluon field* dynamics, i.e., the dynamics in the early stage of HIC. They emphasized that the field fluctuation at the initial state is crucial for the entropy production even when Glasma-like initial conditions are adopted.

While the early stage of HIC should be well described as a classical system, the system *is* nothing more than a quantum system  $|G\rangle$  for which the gluon field  $\hat{A}_\mu^a$  has an expectation value  $A_{c\mu}^a$ ;  $\hat{A}_\mu^a = A_{c\mu}^a + \hat{a}_\mu^a$  where  $A_{c\mu}^a = \langle G | \hat{A}_\mu^a | G \rangle$  and  $|A_{c\mu}^a| \gg |\hat{a}_\mu^a|$  in some measure. The quantum statistical entropy is given by the von Neumann entropy  $S \equiv -\text{Tr} \rho \log \rho$ , with  $\rho$  being the density matrix of the system. Our idea is that the quantum state of the gluon fields in the initial stage of HIC may be well described by a coherent state [25];  $|G\rangle \simeq |\text{coh}\rangle$ , where the coherent state  $|\text{coh}\rangle$  is given solely in terms of the classical fields  $A_{c\mu}^a$ ; the explicit construction of  $|\text{coh}\rangle$  is given in the next section. Then the time evolution of the

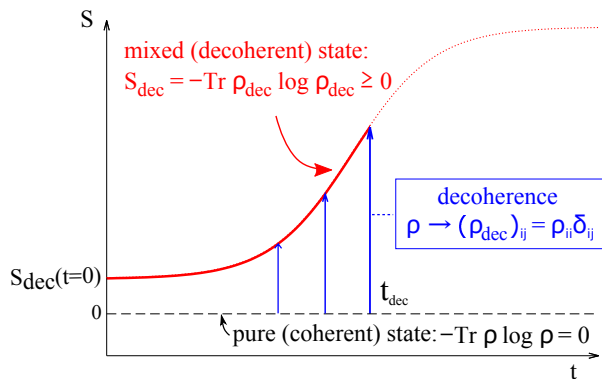


FIG. 1: Schematic illustration of the possible decoherence entropy production process. The red line shows the amount of entropy  $S_{\text{dec}}(t)$  to be liberated at time  $t$  provided that a complete decoherence occurs there, whereas the dashed-black line is the entropy for a pure state. The time evolution of the system is assumed to be described as that of a coherent state until a time  $t_{\text{dec}}$  when decoherence takes place; then the density matrix becomes diagonal so that the von Neumann entropy becomes positive. A possible time-dependence of entropy after  $t_{\text{dec}}$  is expressed by the dotted-red line.

density matrix and hence the von Neumann entropy can be obtained from the classical dynamics.

However, the things do not go so easy: Information loss of the system is indispensable for the entropy production. Indeed, if the system stays in a pure state, where the time evolution is given by a unitary operator, the entropy keeps zero value, as is well known. Thus the system must be or turn to a mixed state to produce the entropy. The conversion from a pure to mixed state or decoherence may be achieved through the interaction of the system with its environment [26]. The decoherence process can be nicely described in terms of the density matrix  $\rho$ ; the nondiagonal elements tends to vanish while the diagonal elements of  $\rho$  becomes semi-positive definite in certain representation in the course of decoherence.

In Refs. [27–29], an estimate of the decoherence time  $\tau_{\text{dec}}$  of the gluon ensemble in HIC is given in a leading-order approximation, and it is argued that  $\tau_{\text{dec}} \sim Q_s^{-1}$ , where  $Q_s$  is the saturation scale of the collision. They also estimate the amount of entropy production during the decoherence from the number of decohering gluons per a coherent domain [30], and found that the produced entropy is roughly one-third of that measured in the final hadron distribution.

In the present paper, we propose a new method for the calculation of the entropy in the initial stage of HIC on the basis of a new scenario of the entropy production by decoherence. As is illustrated in Fig. 1, we assume that there is a stage where the gluon system evolves quantum-mechanically from Glasma initial conditions before the occurrence of the decoherence at a time  $t_{\text{dec}}$ : The gluon system is assumed to be described by a coherent state as in Refs. [27–29], and the time dependence of the expecta-

tion value of gauge fields by the coherent state is obtained from that of the classical gluon fields. In this study, we do not refer to any specific process of the decoherence in the study, and simply assume that a complete decoherence occurs at  $t_{\text{dec}}$ . Then the density matrix becomes diagonal in the gluon Fock state basis  $(\rho_{\text{dec}})_{ij} = \rho_{ii}\delta_{ij}$ , whose diagonal matrix elements are given in terms of the time-dependent coherent state, and thereby we can calculate the von Neumann entropy of the system from the diagonalized decoherent density matrix  $\rho_{\text{dec}}$  constructed from CYM dynamics, its best quantum analogue (the time-dependent coherent states), and the decoherence assumption. Notice that the entropy obtained through a completed decoherence gives a maximum one produced by a possible decoherence of a coherent state. This kind of entropy is referred to as “decoherence entropy”, because the diagonalization of the density matrix is caused by decoherence of a quantum state [26].

As is mentioned above, the chaotic behavior of gluon fields is related to the production of KS entropy, and the fluctuation of the initial state is crucial for the production [16, 17]. As we will see, longitudinal fluctuations in the Glasma initial conditions make the von Neumann entropy much larger, as is the case for Kolmogorov-Sinai entropy. This indicates that the initial fluctuation of classical chromo-electric and magnetic fields is crucial for the production of the entropy, and the production of the entropy would explain the early thermalization.

The paper is organized as follows. In Sec. IIA, the formalism of calculations of time dependence of gauge fields and electric fields is given in the non-compact formalism[16, 17]. In Sec. IIB, basic ingredients for coherent states are presented. The von Neumann entropy defined by a density matrix is introduced here. The setup of initial conditions in a non-expanding geometry which mimics the Glasma initial condition is illustrated in Sec. IIC. In Sec. III, numerical calculations of the time dependence of the entropy with various longitudinal fluctuations are shown. The time dependence of squared electric fields are also shown to see the isotropization of the system. Section IV is devoted to summarize and conclude the present work.

## II. DECOHERENCE ENTROPY FROM CLASSICAL YANG-MILLS DYNAMICS

### A. Formulation of classical Yang-Mills dynamics

First, we briefly give our formulation of calculational scheme of the CYM dynamics. The details can be found in Ref.[16, 17]. In pure Yang-Mills theory in the temporal gauge  $A_0^a = 0$ , the Hamiltonian in the non-compact

( $A$ ,  $E$ ) scheme takes the following form on the lattice

$$H = \frac{1}{2} \sum_{x,a,i} E_i^a(x)^2 + \frac{1}{4} \sum_{x,a,i,j} F_{ij}^a(x)^2, \quad (1)$$

$$F_{ij}^a(x) = \partial_i A_j^a(x) - \partial_j A_i^a(x) + \sum_{b,c} f^{abc} A_i^b(x) A_j^c(x), \quad (2)$$

where  $\partial_i$  is the central difference operator in the  $i$ -direction,  $\partial_i A_j(x) \equiv \{A_j(x + \hat{i}) - A_j(x - \hat{i})\}/2$ , and  $f^{abc}$  is the structure constant. In this study, we deal with SU(2) gauge theory, i.e.,  $f^{abc} = \epsilon^{abc}$ , where  $\epsilon^{abc}$  is the Levi-Civita tensor with  $\epsilon^{123} = +1$ . Note that all the quantities in the equations are given in the lattice unit and thus dimensionless. From Eqs. (1) and (2), we obtain the classical equations of motion (EOM) for the canonical coordinate  $A_i^a(x)$  (gauge fields) and the canonical momentum  $E_i^a(x)$  (color electric fields),

$$\dot{A}_i^a(x) = E_i^a(x), \quad (3)$$

$$\dot{E}_i^a(x) = \sum_j \partial_j F_{ji}^a(x) + \sum_{b,c,j} f^{abc} A_j^b(x) F_{ji}^c(x), \quad (4)$$

which we solve with CGC-like initial conditions to be specified later. The fourth-order Runge-Kutta method is adopted to solve the EOM. We check that the violation of Gauss' law is not harmful for our numerical simulation in the non-compact formalism: the number of positive, negative and zero Lyapunov exponents exists in equal amount (for details, see the appendix of Ref.[17]).

### B. CYM coherent state, decoherence, and von Neumann entropy

Here we give the calculational method of a von Neumann entropy in the initial stage of HIC.

To begin with, as an example, we consider a one-degrees-of-freedom system described by the Hamiltonian  $H = p^2/2m + m\omega^2 q^2/2$ , where  $q$  and  $p$  are the canonical coordinate and momentum. We set  $\hbar = 1$  in the following. The creation and annihilation operators are defined by  $a^\dagger = \sqrt{\frac{m\omega}{2}}(q - ip/m\omega)$  and  $a = \sqrt{\frac{m\omega}{2}}(q + ip/m\omega)$ , respectively, and satisfy  $[a, a^\dagger] = 1$ . Using the creation operator, a Fock state is expressed by  $|n\rangle \equiv \frac{1}{\sqrt{n!}}(a^\dagger)^n|0\rangle$ , and is normalized as  $\langle n|n'\rangle = \delta_{n,n'}$ .

A coherent state  $|\alpha\rangle$  is an eigenstate of an annihilation operator  $a$ , i.e.,  $a|\alpha\rangle = \alpha|\alpha\rangle$ , where the coherent state is normalized as  $\langle\alpha|\alpha\rangle = 1$ . The eigenvalue  $\alpha$  of the coherent state  $|\alpha\rangle$  is written by the expectation value of the coordinate  $q$  and the momentum  $p$  as

$$\alpha = (m\omega\langle\alpha|q|\alpha\rangle + i\langle\alpha|p|\alpha\rangle)/\sqrt{2m\omega}. \quad (5)$$

Such a coherent state can be realized as the superposition of Fock states,

$$|\alpha\rangle = \exp(-|\alpha|^2/2) \sum_{n=0}^{\infty} \frac{\alpha^n}{\sqrt{n!}} |n\rangle. \quad (6)$$

The probability of finding the  $n$ -particle state in the coherent state is then given by

$$P(n) \equiv |\langle n|\alpha\rangle|^2 = \exp(-|\alpha|^2) |\alpha|^{2n}/n!, \quad (7)$$

which is a Poisson distribution. The average particle number  $\bar{n}$  is then written as

$$\bar{n} \equiv \sum_n n |\langle n|\alpha\rangle|^2 = |\alpha|^2. \quad (8)$$

We now proceed with the case of QCD, which has infinite degrees of freedom. The coherent states of gluons have color ( $a$ ), direction ( $i$ ) and momentum indices ( $\vec{k}$ ), i.e.,

$$a_{\vec{k}}^{ia} |\alpha_{\vec{k}}^{ai}\rangle = \alpha_{\vec{k}}^{ia} |\alpha_{\vec{k}}^{ai}\rangle. \quad (9)$$

Thus the eigenvalue  $\alpha_{\vec{k}}^{ai}$  is the expectation value of an annihilation operator  $a_{\vec{k}}^{ia}$  and is expressed by the expectation values of gauge fields and electric fields: The gauge fields  $A^{ai}(\vec{x})$  and electric fields  $E^{ai}(\vec{x})$  are expressed in terms of creation and annihilation operators,  $a_{\vec{k}}^{ai\dagger}$  and  $a_{\vec{k}}^{ai}$ , as

$$A^{ai}(\vec{x}) = \frac{1}{V} \sum_{\vec{k}} \frac{1}{\sqrt{2\omega_{\vec{k}}}} \left\{ e^{i\vec{k}\vec{x} - i\omega t} a_{\vec{k}}^{ai} + e^{-i\vec{k}\vec{x} + i\omega t} a_{\vec{k}}^{ai\dagger} \right\},$$

$$E^{ai}(\vec{x}) = \frac{1}{V} \sum_{\vec{k}} \frac{-i\omega_{\vec{k}}}{\sqrt{2\omega_{\vec{k}}}} \left\{ e^{i\vec{k}\vec{x} - i\omega t} a_{\vec{k}}^{ai} - e^{-i\vec{k}\vec{x} + i\omega t} a_{\vec{k}}^{ai\dagger} \right\}. \quad (10)$$

Here,  $\omega_{\vec{k}}$  on the lattice is defined by

$$\omega_{\vec{k}} \equiv \sqrt{\sin^2 k_x + \sin^2 k_y + \sin^2 k_z}, \quad (11)$$

$$\vec{k} \equiv \left( \frac{2\pi n_x}{N_x}, \frac{2\pi n_y}{N_y}, \frac{2\pi n_z}{N_z} \right), \quad (12)$$

$$0 \leq n_i \leq N_i - 1, n_i \in \mathbb{Z} \quad (i = x, y, z), \quad (13)$$

where  $N_i$  is the number of lattice points in the  $i$ -direction. The expectation values of gauge and electric fields for coherent states are then expressed as

$$\langle A^{ai}(\vec{x}) \rangle = \frac{1}{V} \sum_{\vec{k}} \frac{1}{\sqrt{2\omega_{\vec{k}}}} \left\{ e^{i\vec{k}\vec{x} - i\omega t} \langle a_{\vec{k}}^{ai} \rangle + e^{-i\vec{k}\vec{x} + i\omega t} \langle a_{\vec{k}}^{ai\dagger} \rangle \right\},$$

$$\langle E^{ai}(\vec{x}) \rangle = \frac{1}{V} \sum_{\vec{k}} \frac{-i\omega_{\vec{k}}}{\sqrt{2\omega_{\vec{k}}}} \left\{ e^{i\vec{k}\vec{x} - i\omega t} \langle a_{\vec{k}}^{ai} \rangle - e^{-i\vec{k}\vec{x} + i\omega t} \langle a_{\vec{k}}^{ai\dagger} \rangle \right\}. \quad (14)$$

In the momentum space, these expectation values are written as

$$\langle A^{ai}(\vec{k}) \rangle = (\langle a_{\vec{k}}^{ai} \rangle + \langle a_{\vec{k}}^{ai\dagger} \rangle) / \sqrt{2\omega_{\vec{k}}}, \quad (15)$$

$$\langle E^{ai}(\vec{k}) \rangle = (-i\omega_{\vec{k}}) (\langle a_{\vec{k}}^{ai} \rangle - \langle a_{\vec{k}}^{ai\dagger} \rangle) / \sqrt{2\omega_{\vec{k}}}. \quad (16)$$

From the above equations, the eigenvalue  $\alpha_{\vec{k}}^{ai}$ , i.e., the expectation value of the annihilation operator, is expressed as

$$\alpha_{\vec{k}}^{ai} = \langle a_{\vec{k}}^{ai} \rangle = \frac{1}{\sqrt{2\omega_{\vec{k}}}} (\omega_{\vec{k}} \langle A^{ai}(\vec{k}) \rangle + i \langle E^{ai}(\vec{k}) \rangle). \quad (17)$$

The corresponding expansion of coherent states  $|\alpha_{\vec{k}}^{ai}\rangle$  by Fock states  $|n, a, i, \vec{k}\rangle$  is written as

$$|\alpha_{\vec{k}}^{ai}\rangle = \exp(-|\alpha_{\vec{k}}^{ai}|^2/2) \sum_{n=0}^{\infty} \frac{\alpha_{\vec{k}}^{ai n}}{\sqrt{n!}} |n, a, i, \vec{k}\rangle. \quad (18)$$

The probability of finding the  $n$ -particle state,  $P_{\vec{k}}^{ai}(n)$  in the coherent state is given by

$$P_{\vec{k}}^{ai}(n) \equiv |\langle n, a, i, \vec{k} | \alpha \rangle|^2 = \exp(-|\alpha_{\vec{k}}^{ai}|^2) |\alpha_{\vec{k}}^{ai}|^{2n} / n!. \quad (19)$$

Also, the average particle number  $\bar{n}_{\vec{k}}^{ai}$  is

$$\bar{n}_{\vec{k}}^{ai} \equiv \sum_n n |\langle n, a, i, \vec{k} | \alpha_{\vec{k}}^{ai} \rangle|^2 = |\alpha_{\vec{k}}^{ai}|^2. \quad (20)$$

Because  $\langle A^{ai}(\vec{k}) \rangle$  and  $\langle E^{ai}(\vec{k}) \rangle$  are the expectation values for coherent states, which are the best quantum analogue of classical observables, *we substitute the classical fields  $A^{ai}(\vec{k})$  and  $E^{ai}(\vec{k})$  obtained by solving CYM equation for  $\langle A^{ai}(\vec{k}) \rangle$  and  $\langle E^{ai}(\vec{k}) \rangle$* , which enables us to compute the time dependence of  $\alpha_{\vec{k}}^{ai}$  with CYM.

From the coherent states of gluon fields, we can evaluate the density matrix  $\rho$  and the von Neumann entropy after decoherence as follows. The gluon state is assumed to be a direct product of gluon coherent state in the calculation,

$$\rho = \prod_{a,i,\vec{k}} |\alpha_{\vec{k}}^{ai}\rangle \langle \alpha_{\vec{k}}^{ai}|.$$

The density matrix for a certain  $\vec{k}, a$  and  $i$  can be written as

$$\rho_{m,n}^{ai\vec{k}} = \langle m, ai\vec{k} | \alpha_{\vec{k}}^{ai} \rangle \langle \alpha_{\vec{k}}^{ai} | n, ai\vec{k} \rangle, \quad (21)$$

where  $|m, ai\vec{k}\rangle$  is a Fock state with particle number  $m$ , color  $a$ , direction  $i$  and momentum  $\vec{k}$ . A von Neumann entropy is defined as

$$S = -\text{Tr}(\rho \ln \rho). \quad (22)$$

For a pure state, the entropy is zero, because the pure state condition  $\rho^2 = \rho$  results in the eigenvalues of  $\rho$  of 0 or 1. As is mentioned in Introduction, we assume a complete decoherence at a time, and then the density matrix becomes diagonal in the gluon Fock state basis  $|n, ai\vec{k}\rangle$  as

$$(\rho_{\text{dec}})_{m,n}^{ai\vec{k}} = \rho_{nn}^{ai\vec{k}} \delta_{mn} = P_{\vec{k}}^{ai}(n) \delta_{mn}, \quad (23)$$

and the von Neumann entropy becomes nonzero,

$$\begin{aligned} S_{\text{dec}} &= -\text{Tr}(\rho_{\text{dec}} \ln \rho_{\text{dec}}) \\ &= -\sum_{n,a,i,\vec{k}} P_{\vec{k}}^{ai}(n) \ln P_{\vec{k}}^{ai}(n) \geq 0. \end{aligned} \quad (24)$$

This entropy is referred to as ‘‘decoherence entropy’’, as mentioned in Introduction.

### C. Initial conditions with coherent background fields

One of the realistic initial conditions of high-energy heavy-ion collisions is so-called Glasma [6, 7, 31, 32], where both the color-electric and -magnetic fields are parallel to the collision axis. In this study, we adopt a Glasma-like initial condition (GIC) in the non-expanding geometry, which is explained below.

The Glasma initial condition describes the gauge fields at proper time  $\tau \equiv \sqrt{t^2 - z^2} = 0^+$ , when two nuclei move along  $z$  axis almost at the speed of light and collide at  $t = 0$  and  $z = 0$ . The gluons having large Bjorken  $x$  and quarks are assumed to be color sources for low  $x$  gluons in the initial condition. The model in which the color-source distribution is Gaussian is called McLerran-Venugopalan model [6].

We prepare an initial condition which mimics the MV model in the non-expanding geometry: The color sources which obey Gaussian distribution are set and then electric fields and magnetic fields aligned in the collision axis are generated from the sources. The small fluctuations in the  $z$  direction is also added on the above fields as in Ref. [7].

The procedure to generate color-electric and -magnetic fields is given as follows:

- Generate the Gaussian random color sources for a target nucleus  $\rho^{(t)}$  and a projectile  $\rho^{(p)}$  which satisfies
 
$$\langle \rho^{(t)a}(\mathbf{x}_{\perp}) \rho^{(t)b}(\mathbf{y}_{\perp}) \rangle = g^4 \mu^2 \delta^{ab} \delta^{(2)}(\mathbf{x}_{\perp} - \mathbf{y}_{\perp})$$
 and
 
$$\langle \rho^{(p)a}(\mathbf{x}_{\perp}) \rho^{(p)b}(\mathbf{y}_{\perp}) \rangle = g^4 \mu^2 \delta^{ab} \delta^{(2)}(\mathbf{x}_{\perp} - \mathbf{y}_{\perp}),$$
 where  $\mathbf{x}_{\perp} \equiv (x, y)$  and  $a, b$  are the color indices.
- Solving the Poisson equations:
 
$$-\partial_{\perp}^2 \Lambda^{(t)}(\mathbf{x}_{\perp}) = \rho^{(t)}(\mathbf{x}_{\perp}),$$

$$-\partial_{\perp}^2 \Lambda^{(p)}(\mathbf{x}_{\perp}) = \rho^{(p)}(\mathbf{x}_{\perp})$$
- Wilson lines are calculated as
 
$$V^{\dagger}(\mathbf{x}_{\perp}) = e^{i\Lambda^{(t)}(\mathbf{x}_{\perp})}, \quad W^{\dagger}(\mathbf{x}_{\perp}) = e^{i\Lambda^{(p)}(\mathbf{x}_{\perp})}.$$
- Gauge fields are given by  $\alpha_i^{(t)} = iV\partial_i V^{\dagger}$  ( $i = x, y$ ) and  $\alpha_i^{(p)} = iW\partial_i W^{\dagger}$ .
- From  $\alpha_i^{(t)}$  and  $\alpha_i^{(p)}$ , gauge fields are constructed as

$$A^i = \alpha_i^{(t)} + \alpha_i^{(p)}, \quad A^z = 0. \quad (25)$$

Electric fields and magnetic fields are then given by

$$E^i = 0, E^z = i \sum_i \left( \left[ \alpha_i^{(t)}, \alpha_i^{(p)} \right] \right), \quad (26)$$

$$B^i = 0, B^z = i \left( \left[ \alpha_1^{(t)}, \alpha_2^{(p)} \right] + \left[ \alpha_1^{(p)}, \alpha_2^{(t)} \right] \right). \quad (27)$$

The initial condition gives electric fields and magnetic fields parallel to the  $z$  direction and have fluctuations in the  $x$  and  $y$  directions.

We also include fluctuations in the  $z$  direction as follows [7]:

- Generate the Gaussian random fluctuations of electric fields,  $\delta \bar{E}_i(\mathbf{x}_\perp)$ , which satisfies

$$\langle \delta \bar{E}_i(\mathbf{x}_\perp) \delta \bar{E}_j(\mathbf{y}_\perp) \rangle = \delta_{ij} \delta(\mathbf{x}_\perp - \mathbf{y}_\perp) \quad (28)$$

and also fluctuations in  $z$  direction  $F(z)$  satisfying

$$g^2 \mu \langle F(z) F(z') \rangle = \Delta^2 \delta(z - z'). \quad (29)$$

- $E^i(\mathbf{x}_\perp, z)$  and  $E^z(\mathbf{x}_\perp, z)$  are composed from these fluctuations as

$$E^i(\mathbf{x}_\perp, z) = \delta E_i(\mathbf{x}_\perp, z), \quad (30)$$

$$\begin{aligned} E^z(\mathbf{x}_\perp, z) &= i \sum_i \left( \left[ \alpha_i^{(t)}, \alpha_i^{(p)} \right] \right) + \delta E_z(\mathbf{x}_\perp, z) \\ &\equiv E_z^{(0)} + \delta E_z(\mathbf{x}_\perp, z), \end{aligned} \quad (31)$$

where

$$\delta E_i(\mathbf{x}_\perp, z) = \partial_z F(z) \delta \bar{E}_i(\mathbf{x}_\perp), \quad (32)$$

$$\delta E_z(\mathbf{x}_\perp, z) = -F(z) D_i \delta \bar{E}_i(\mathbf{x}_\perp), \quad (33)$$

and  $E_z^{(0)}$  is the electric field without fluctuations shown in Eq. (26)

GIC shown in Eqs. (25), (30) and (31) with  $(t, \mathbf{x}_\perp, z)$  coordinates are given in almost the same way as those in the original formulation, which is given in an expanding geometry with  $(\tau, \mathbf{x}_\perp, \eta)$  coordinates [6, 7, 31, 32], by replacing  $(\tau, \eta)$  with  $(t, z)$ . Since we replace  $\delta(\eta - \eta')$  in an expanding geometry with  $\delta(z - z')$  in a non-expanding geometry in Eq. (29), we have introduced a scale factor  $g^2 \mu$  in Eq. (29) in order to compensate the dimension coming from  $\delta(z - z')$ . It should be noted that the present initial condition does not have the connection with the color glass condensate wave function of the colliding nuclei. We remark that the construction of electric fields is consistent with Gauss' law,  $D_i E^i + D_z E^z = 0$ .

### III. DECOHERENCE ENTROPY FROM GLASMA INITIAL CONDITION

In this section, we show the numerical results of the entropy evaluated with GIC. Note that we set  $g^2 \mu = 1$  in

TABLE I: Parameter set for the Glasma initial conditions.  $\Delta$  denotes the amplitude of longitudinal fluctuations,  $\epsilon$  is energy density written in  $(g^2 \mu)^4$  and  $\text{GeV}/\text{fm}^3$ , and ‘‘ratio of  $E^2$ ’’ is defined by  $\sum_{\vec{x}, a} \delta E_z^a(\vec{x})^2 / \sum_{\vec{x}, a} E_z^{(0)a}(\vec{x})^2$ , where  $\delta E_z^a(\vec{x})$  and  $E_z^{(0)a}(\vec{x})$  are defined in Eq.(31). The physical scale of energy density is determined by regarding the transverse area of the lattice as a section of an Au nucleus (see the last paragraph of Sec.III).

volume	$\Delta$	$\epsilon(g^2 \mu)^4$	$\epsilon(\text{GeV}/\text{fm}^3)$	ratio of $E^2$
$20^3$	0	0.1711	0.3476	0
$20^3$	$1.0 \times 10^{-3}$	0.1711	0.3476	$3.278 \times 10^{-5}$
$20^3$	$5.0 \times 10^{-3}$	0.1712	0.3478	$8.194 \times 10^{-4}$
$20^3$	$1.0 \times 10^{-2}$	0.1714	0.3482	$3.278 \times 10^{-3}$
$20^3$	$5.0 \times 10^{-2}$	0.1814	0.3685	$8.194 \times 10^{-2}$
$20^3$	$1.0 \times 10^{-1}$	0.21	0.4266	$3.278 \times 10^{-1}$

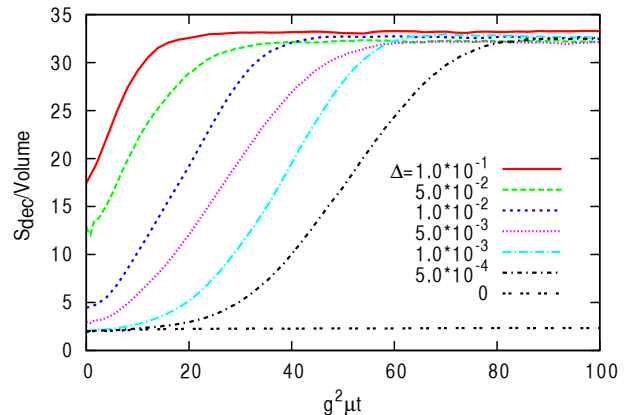


FIG. 2: Time dependence of density of the entropy,  $S_{\text{dec}}/\text{Volume}$ , from Glasma initial condition with various fluctuations  $\Delta$  in  $z$  direction shown in Eq.(29).

the numerical calculation. In Table I, parameters used in the initial condition are summarized; volume, amplitudes of longitudinal fluctuations, and initial energy densities. We also show the squared fluctuation-background electric field ratio defined by  $\sum_{\vec{x}, a} \delta E_z^a(\vec{x})^2 / \sum_{\vec{x}, a} E_z^{(0)a}(\vec{x})^2$ , where  $\delta E_z^a(\vec{x})$  and  $E_z^{(0)a}(\vec{x})$  are defined in Eq. (31).

Figure 2 shows the time dependence of the entropy density,  $S_{\text{dec}}/\text{Volume}$ , from GIC with fluctuations in the  $z$  direction. The amplitude of longitudinal fluctuations,  $\Delta$  in Eq.(29), varies from 0 to  $1.0 \times 10^{-1}$ . The lines correspond to different amplitudes of longitudinal fluctuations,  $\Delta$ . We will mention the choice of the amplitudes  $\Delta$  later. With  $\Delta = 0$ , the entropy is almost constant:  $S_{\text{dec}}/\text{Volume} \simeq 2.3$  for our calculation time,  $g^2 \mu t < 100$ . On the other hand, with finite  $\Delta$ ,  $S_{\text{dec}}/\text{Volume}$  starts to increase at a certain time. For example, with  $\Delta = 5.0 \times 10^{-4}$ ,  $S_{\text{dec}}/\text{Volume}$  is almost the same as that without fluctuation for  $g^2 \mu t < 18$ , and it starts to increase after that and saturates around  $g^2 \mu t = 80$ . The onset

time of entropy increase becomes earlier as the fluctuation  $\Delta$  becomes larger. For  $\Delta > 5.0 \times 10^{-3}$ ,  $S_{\text{dec}}/\text{Volume}$  at the initial time is already larger than that without fluctuations. Thus, we find the two kinds of origin of the entropy. One is the non-linear dynamics of CYM, which is triggered by small fluctuations after a certain time. The other is the intrinsic entropy which is potentially prepared in the initial state (at  $t = 0$ ).

We here discuss the relation between time dependence of the entropy and the initial fluctuations. In the previous paper [16, 17], chaotic behavior of CYM and the entropy production are studied. They find that the instability and chaotic behavior of CYM are the origin of the Kolmogorov-Sinai (KS) entropy, which is obtained by the sum of positive Lyapunov exponents and shows the entropy production rate. On the other hand, the entropy itself is studied here. The numerical results obtained here indicate that the production of the decoherence entropy would be also related to instabilities and chaoticity of the system. Without longitudinal fluctuations, i.e., the amplitude  $\Delta = 0$ , no long-standing instability exists. While the initial Glasma configuration has a potential instability in the longitudinal fluctuation direction leading to macroscopic number of the Kolmogorov-Sinai entropy obtained as the sum of positive Lyapunov exponents, actual entropy production would not be realized because of the translational invariance in  $z$  direction. The number of excited modes is that of two-dimensional lattice, and dimensionally reduced entropy from two-dimensional chaos is realized. With finite  $\Delta$ , potential instability represented as positive Lyapunov exponents is manifested, and full 3-dimensional entropy production is realized. The number of degrees of freedom is proportional to the lattice sites, and the entropy is roughly about  $N_z$  times larger than that in the  $\Delta = 0$  case, where  $N_z$  is the lattice size in  $z$  direction and  $N_z = 20$  in the present calculation. Our results show that the entropy with finite  $\Delta$  is around 16 times larger than that with  $\Delta = 0$ , which is 80% of the expected ratio. This small reduction is understood as the difference of the distribution of the average particle number  $\bar{n}_k^{ai}$ . With  $\Delta = 0$ , energy is concentrated in smaller number of modes, and we find  $\bar{n}$  is larger in excited modes,  $\alpha \neq 0$ , then the entropy per excited mode is slightly larger with  $\Delta = 0$ .

Next, we discuss isotropization of the system. In general, the isotropization time depends on physical observables. We here examine squared electric fields in the perpendicular and the longitudinal directions,  $E_{\text{perp}}^2 = ((E^{xa})^2 + (E^{ya})^2)/2$  and  $E_{\text{long}}^2 = (E^{za})^2$ . The upper panel of Fig.3 shows  $E_{\text{perp}}^2$  and  $E_{\text{long}}^2$  computed without fluctuations in the initial fields' configuration. Initially, there is finite  $E_{\text{long}}^2$  and no  $E_{\text{perp}}^2$ . As time goes by,  $E_{\text{perp}}^2$  grows and  $E_{\text{long}}^2$  become small. However, they do not coincide for  $g^2\mu t < 50$  as seen from the figure. The lower panel of Fig.3 shows  $E_{\text{perp}}^2$  and  $E_{\text{long}}^2$  estimated with initial longitudinal fluctuations, where the amplitudes of the fluctuation,  $\Delta$ , are 0.1 and 0.05. While for

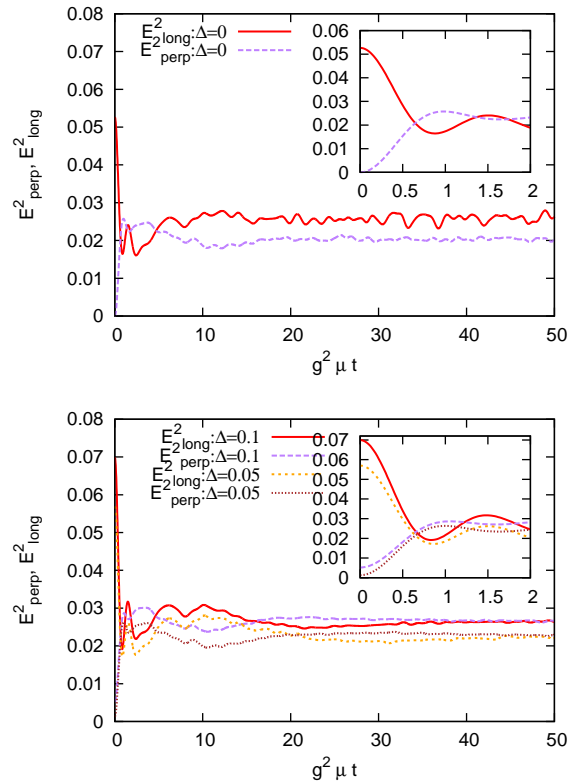


FIG. 3: (Upper figure): time evolution of  $E_{\text{perp}}^2$  and  $E_{\text{long}}^2$  from the Glasma initial conditions without fluctuations. (Lower figure): that with fluctuations ( $\Delta = 0.1$  and  $0.05$ ). The figures in the right-top side of the two figures are the enlarged views of each figure for  $t = 0$  to  $2(g^2\mu)^{-1}$

$\Delta = 0.1$ , the initial behavior of those are similar to that without fluctuations,  $E_{\text{perp}}^2$  and  $E_{\text{long}}^2$  almost coincides after  $g^2\mu t \simeq 35$ , which indicates isotropization of the system. For  $\Delta = 0.05$ , the basic behavior is the same as that for  $\Delta = 0.1$ , but the isotropization time is a bit longer than that with  $\Delta = 0.1$ :  $g^2\mu t \simeq 40$  for this amplitude, which indicates the stronger fluctuations cause faster isotropization. We note that the ‘‘isotropization’’ here is determined by that of electric fields, and there might be some quantities that is not isotropized after the isotropization of electric fields.

We briefly comment on the choice of the range of fluctuations,  $0 < \Delta < 1.0 \times 10^{-1}$ . Since the longitudinal fluctuation strength is of order  $g^2$  compared to the background field in the perturbative regime, longitudinal fluctuations should not be large. As shown in Table I, the squared fluctuation-background electric field ratio,  $\sum_{\vec{x}, a} \delta E_z^a(\vec{x})^2 / \sum_{\vec{x}, a} E_z^{(0)a}(\vec{x})^2$ , is less than  $1/3 \times 10^{-1}$ . The fluctuations with  $\Delta \leq 0.1$  are judged to be small compared with the background field and thus these fluctuations are acceptable.

Rough estimation of the physical scale can be done by regarding the transverse area of the lattice as a section of

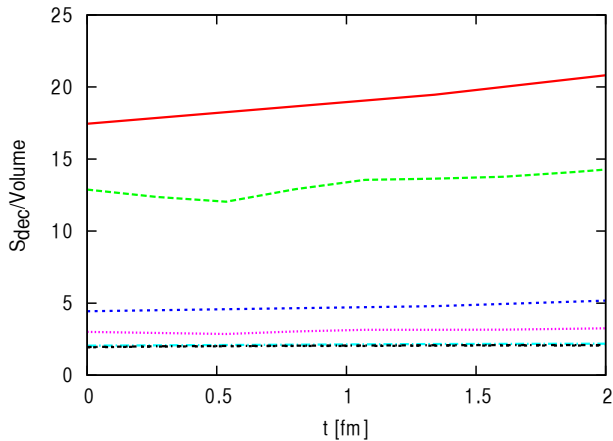


FIG. 4: The same figure of Fig.2 with a physical scale in the horizontal axis for  $t=0$  to 2fm. The lines correspond to different amplitudes of longitudinal fluctuations,  $\Delta$ , and the correspondence of line types with  $\Delta$  is the same as that of Fig.2. Note that three lines for  $\Delta = 0, 5.0 \times 10^{-4}$  and  $1.0 \times 10^{-3}$  are almost degenerate in the time interval.

an Au nucleus. This enables us to determine the physical length of the lattice,  $L$ , as  $L^2 \simeq \pi R_{\text{Au}}^2$  with the radius of an Au nucleus,  $R_{\text{Au}} \simeq 7\text{fm}$ . The resulting physical length is  $L \simeq 12.4\text{fm}$ . From the present lattice extent  $g^2\mu L = 20$ , we obtain  $g^2\mu \simeq 0.32\text{GeV} \simeq (0.63\text{fm})^{-1}$ . Figure 4 is the same as Fig.2 but with the horizontal axis from  $t=0$  to 2fm. From the figure, we see that the entropy is roughly constant in the time interval, which implies the importance of the potential entropy possessed in the initial state and the decoherence time at which the decoherence entropy is realized for the understanding of early thermalization. We should note here that the determination of the physical scale has large uncertainty and we also do not know how large the actual longitudinal fluctuation is. Further study is necessary for the deeper understanding of the entropy production.

#### IV. SUMMARY AND CONCLUSION

We have studied entropy production in the initial stage of HIC. We have proposed a method to compute (quantum mechanical) von Neumann entropy utilizing the dynamics of classical Yang-Mills(CYM) fields under the following two assumptions: One is that the gluon state in the initial stage is well represented by a quantum coherent state, and the time evolution of the classical gluon fields as given by the expectation values of the coherent state is provided by the CYM dynamics. The other is that the density matrix becomes fully diagonal, i.e., complete decoherence occurs at a time  $t_{\text{dec}}$ , which gives the upper limit of the entropy produced through decoherence. The von Neumann entropy evaluated here is referred to as the decoherence entropy. We do not specify

the mechanism of the decoherence here. We have adopted an initial condition, Glasma-like initial condition (GIC), which mimics the Glasma in the non-expanding geometry to calculate the time dependence of the entropy. The longitudinal fluctuation is imposed to the initial condition and we see the dependence of the entropy production on the longitudinal fluctuations.

In GIC with small longitudinal fluctuations, the entropy starts to increase at a certain time and is enhanced compared with that without longitudinal fluctuations. The onset time of the entropy increase depends on the ratio of the fluctuations to background color-electric and magnetic fields. Thus, the longitudinal fluctuations in the initial condition are quite important for entropy production. On the other hand, with large longitudinal fluctuations, the decoherence entropy is already large at  $t = 0$ . We find two kinds of origin of the entropy: One is the non-linear dynamics of CYM triggered by small fluctuations after a certain time, and the other is the intrinsic entropy potentially kept in the initial state.

We have discussed the relation between the production of the decoherence entropy and the instability and chaoticity of the system. Without the longitudinal fluctuations, the instability in the longitudinal direction is not realized due to translational invariance in longitudinal direction and the entropy production is dimensionally reduced. On the other hand, a full 3-dimensional entropy production is realized by the longitudinal fluctuations due to the realization of instability and chaoticity in the longitudinal direction. Our numerical simulations support the scenario.

Isotropization has also been investigated via squared electric fields. We find that isotropization of the system in GIC is also intimately related to the fluctuation of electric and magnetic fields in the initial stage. We have also estimated the physical scale and find that the initial entropy kept in the coherent state and the decoherence time would be important for the understanding of the early thermalization. We should note that we still have uncertainty in the determination of the physical scale and the magnitude of longitudinal fluctuations, which should be resolved before drawing phenomenological conclusions.

In the present study, we neglect the expansion of a Glasma along the collision axis. The effect of expansion would make the thermalization slower. Therefore, to include the effect in the calculation is an important future task to understand the entropy production and the thermalization in HIC.

*Acknowledgment.* We are grateful to Berndt Müller for fruitful discussions and making us aware of Refs.[27–29] after the initiation of the present work. The calculations were performed mainly by using the NEC-SX9 at Osaka University. This work was supported in part by Grant-in-Aid for Scientific Research from the Japan Society for the Promotion of Science (JSPS) and the Ministry of Education, Culture, Sports, Science and Technology of Japan (MEXT) (Nos. 20540265 Innovative Areas (No. 2004: 23105713, and No. 2404: 24105001, 24105008),

23340067, 24340054, 24540271), by the Yukawa International Program for Quark-Hadron Sciences, by a Grant-in-Aid for the global COE program “The Next Genera-

tion of Physics, Spun from Universality and Emergence” from MEXT. T. K. is supported by the Core Stage Back UP program in Kyoto University.

- 
- [1] U. Heinz, private communication; R. Chatterjee and D. K. Srivastava, Nucl. Phys. A **830**, 579C (2009).
- [2] U.W.Heinz and P.F.Kolb, Nucl.Phys.**A702**, 269 (2002) [arXiv:hep-ph/0111075].
- [3] R. Baier, A. H. Mueller, D. Schiff and D. T. Son, Phys. Lett. B **502**, 51 (2001) [hep-ph/0009237].
- [4] L.V.Gribov, E.M.Levin and M.G.Ryskin, Nucl. Phys. **B188**, 555-576 (1981); Phys. Rept. **100**, 1-150 (1983).
- [5] A.H.Müller and J-W Qiu, Nucl. Phys. **B268**, 427-452 (1986).
- [6] L.McLerran and R.Venugopalan, Phys. Rev. D**49**, 2233 (1994); *ibid.* **49** 3552 (1994); *ibid.* **50**, 2225 (1994).
- [7] P.Romatschke and R.Venugopalan, Phys. Rev. D**74**, 045011 (2006).
- [8] J. Berges, S. Scheffler, and D.Sexty, Phys. Rev. D**77**, 034504 (2008); J. Berges, S. Scheffler, S. Schlichting and D. Sexty, Phys.Rev.D**85**, 034507 (2012).
- [9] T.Epelbaum and F.Gelis, Phys. Rev. Lett. **111**, 232301.
- [10] E.S.Weibel, Phys.Rev.Lett.**2**, 83 (1959).
- [11] N. K. Nielsen and P. Olesen, Nucl. Phys. B **144**, 376 (1978).
- [12] S. Mrówczyński, Phys. Lett. B **314**, 118 (1993).
- [13] A. Iwazaki, Phys.Rev.C**77**, 034907 (2007).
- [14] H.Fujii and K.Itakura, Nucl. Phys. **A809**, 88 (2008).
- [15] H.Fujii, K.Itakura, and A.Iwazaki, Nucl. Phys. **A828**, 178 (2009).
- [16] T.Kunihiro, B.Müller, A.Ohnishi, A.Schäfer, T.T.Takahashi and A.Yamamoto, Phys. Rev. D**82**, 114015, 2010.
- [17] H.Iida, T.Kunihiro, B.Müller, A.Ohnishi, A.Schäfer and T.T.Takahashi, arXiv:1304.1807.
- [18] For a review of results before 1995 see: T. S. Biró, S. G. Matinyan and B. Müller, *Chaos and gauge field theory*, World Sci. Lect. Notes Phys. **56**, 1 (1994).
- [19] S. G. Matinyan, E. B. Prokhorenko and G. K. Savvidy, JETP Lett. **44**, 138 (1986); Nucl. Phys. B **298**, 414 (1988).
- [20] B. Müller and A. Trayanov, Phys. Rev. Lett. **68**, 3387 (1992).
- [21] J. Bolte, B. Müller and A. Schäfer, Phys. Rev. D **61**, 054506 (2000) [arXiv:hep-lat/9906037].
- [22] T. S. Biró, C. Gong and B. Müller, Phys. Rev. D **52**, 1260 (1995) [arXiv:hep-ph/9409392].
- [23] C. Gong, Phys. Rev. D **49**, 2642 (1994) [arXiv:hep-lat/9308001].
- [24] T. Kunihiro, B. Müller, A. Ohnishi and A. Schäfer, Prog. Theor. Phys. **121**, 555 (2009) [arXiv:0809.4831 [hep-ph]].
- [25] J. Glauber, Phys. Rev. **130**, 2529 (1963).
- [26] W.H.Zurek, Phys. Today **44N10**, 36-44, 1991; arXiv:quant-ph/0306072.
- [27] B.Müller and A.Schäfer, arXiv:hep-ph/0306309.
- [28] B.Müller and A.Schäfer, Phys. Rev. C**73**, 054905 (2006).
- [29] R. J. Fries, B. Müller and A. Schäfer, Phys. Rev. C **79**, 034904 (2009) [arXiv:0807.1093 [nucl-th]].
- [30] Yu. V. Kovchegov, Nucl. Phys. **A692**, 557 (2001).
- [31] K.Fukushima, Acta Phys. Polon. B**42**, 2697-2715 (2011).
- [32] K.Fukushima and F.Gelis, Nucl. Phys. A**874**, 108-129 (2012).